Mon. Not. R. Astron. Soc. **000**, 1–5 (2000) Printed 1 February 2008 (MN LATEX style file v1.4)

Unipolar outflows and global meridional circulations in rotating accretion flows

Igor V. Igumenshchev⋆ †
Institute for Theoretical Physics, Göteborg University and Chalmers University of Technology, 412 96 Göteborg, Sweden

1 February 2008

ABSTRACT

Using two-dimensional simulations of non-radiative viscous rotating black hole accretion flows, we show that the flows with $\alpha \sim 0.1 - 0.3$ self-organize to form stationary unipolar or bipolar outflows accompanied by global meridional circulations. The required energy comes, with efficiency $\sim 0.001 - 0.01$, from the matter directly accreted onto black hole. Observational implications are discussed.

Key words:
accretion: accretion discs — black holes physics — hydrodynamics

1 INTRODUCTION

The considerable recent interest in models of geometrically thick rotating accretion flows has been motivated by ability of these models to explain unusual observational properties of some accreting black hole candidates. There are two major classes of such models. (a) At low accretion rates, the optically thin accretion flow is not able to radiate efficiently and the internal energy stored in the flow is advected into the black hole. Models of such flows have been developed by Ichimaru (1977), Rees et al. (1982), Narayan & Yi (1994), Abramowicz et al. (1995), and others see in recent reviews by Narayan, Mahadevan & Quataert (1998) and Kato, Fukue & Mineshige (1998). These models are called advection dominated accretion flows (ADAFs) and have been applied for explanation of spectral properties of low luminosity high-energy sources. (b) At high accretion rates the flow is optically thick. The liberated binding energy is converted to radiation which is trapped by the flow and advected into the black hole as shown by Katz (1977) and Begelman (1978) for spherical accretion. Rotating accretion flows of this type are called thick discs, Polish doughnuts, or slim discs. They have been developed by Abramowicz, Jaroszyński & Sikora (1978), Jaroszyński, Abramowicz & Paczyński (1980), Abramowicz et al. (1988) and others.

Most of the ADAF models have been constructed in a one-dimensional approach which restricts properties of the solutions by considering only the vertically-averaged purely inward motion: the multidimensional character of flow is missing. Narayan & Yi (1995a) pointed out the possible importance of polar outflows in ADAFs. Analytic study of accretion flows with polar outflows was performed by Xu & Chen (1997) and Blandford & Begelman (1999) in a self-similar approach, and numerical two-dimensional studies have recently been carried out by Igumenshchev, Chen & Abramowicz (1996), Igumenshchev & Abramowicz (1999, hereafter IA99) and Stone, Pringle & Begelman (1999). These numerical studies demonstrated that in the case of small or moderate viscosity ($\alpha \lesssim 0.1$), non-radiative accretion flows are convectively unstable and accompanied by irregular bipolar outflows. They do not form powerful unbound winds. At large viscosity ($0.1 \lesssim \alpha < 1$) flows are stable and may have (but do not have to have) strong outflows.

In this Letter we present results from two-dimension axisymmetric hydrodynamical simulations of non-radiative rotating accretion flows with large viscosity. The flows form powerful unipolar or bipolar outflows and could be stationary or nonstationary, depending both on α and on the adiabatic index γ, and self-organize into global meridional circulation cell(s). The energy required to support the circulation is extracted from matter accreted into the black hole with efficiency $\sim 10^{-3} - 10^{-2}$.

2 NUMERICAL METHOD

We compute models by solving the non-relativistic hydrodynamical equations

$$\frac{d\rho}{dt} + \rho\nabla\vec{v} = 0, \tag{1}$$

$$\rho\frac{d\vec{v}}{dt} = -\nabla P + \rho\nabla\Phi + \nabla\mathbf{\Pi}, \tag{2}$$

⋆ E-mail: ivi@fy.chalmers.se
† On leave from: Institute of Astronomy, 48 Pyatnitskaya street, Moscow, 109017, Russia

Table 1. Parameters of two-dimension models.

Model	α	γ	outflow	stability	ϵ
A	0.3	5/3	bipolar	stable	0.002
B	0.1	5/3	unipolar	stable	0.012
C	0.3	4/3	unipolar	quasi-stable	0.002
D	0.1	4/3	bipolar	unstable	0.006

$$\rho\frac{de}{dt} = -P\nabla\vec{v} + Q, \tag{3}$$

where ρ is the density, $\vec{v}$ is the velocity, $\Phi = -GM/r$ is the Newtonian gravitational potential for a central point mass M, e is the specific internal energy, $\mathbf{\Pi}$ is the viscous stress tensor with all components included, and Q is the dissipation function. We adopt the ideal gas equation of state, $P = (\gamma - 1)\rho e$, and consider only the shear viscosity, assuming the α-prescription,

$$\nu = \alpha\frac{c_s^2}{\Omega_K}, \tag{4}$$

where $c_s = \sqrt{P/\rho}$ is the isothermal sound speed, and $\Omega_K = \sqrt{GM/r^3}$ is the Keplerian angular velocity. Details of the numerical technique used to solve (1)-(3) in axial symmetry were discussed by IA99.

We use a spherical grid $N_r \times N_\theta = 130 \times 50$ with the inner radius at $r_{in} = 3r_g$ and the outer radius at $r_{out} = 8000r_g$, where $r_g = 2GM/c^2$ is the gravitational radius of black hole. The grid extends from 0 to π in the polar direction. To model the relativistic Roche lobe overflow, that governs the flow near to the black hole (Abramowicz 1981), in Newtonian gravity we adopt absorbing boundary conditions at $r = r_{in}$ together with the condition of the derivatives $d(v_\theta/r)/dr$ and $d(v_\phi/r)/dr$ being zero. The latter means that there is no viscous energy flux from the inner boundary associated with the $(r\theta)$ and $(r\phi)$ components of the shear stress. At r_{out} we apply free outflow boundary conditions by interpolating all dynamical variables behind r_{out}.

In the calculations we assume a source of matter with a constant ejection rate. The source is located around $\theta = \pi/2$ in the vicinity of r_{out}. Matter is ejected there with angular momentum equal to 0.95 times the Keplerian angular momentum. Due to the viscous spread, part of the ejected matter moves inwards and forms the accretion flow. The other part leaves the computation domain freely through the outer boundary. We start the computation of a model from an initial state, the choice of which is not crucial, and follow the evolution until a quasi-stationary flow pattern is established. Typically, this takes a few viscous time scales estimated at r_{out}.

3 TWO-DIMENSION HYDRODYNAMICAL MODELS

Four models with various values of α and γ are listed in Table 1, which also lists the type of the outflow, the stability and the efficiency ϵ defined by (8). All of the models have powerful outflows, launched at radial distances $10 - 100r_g$. Models A and B are stationary, and Model C shows a stable time-averaged global flow pattern, perturbed from time to time by hot convective bubbles that originate very close to r_{in}. Model D is less stationary, with significant convection activity which originates in the innermost part of the flow.

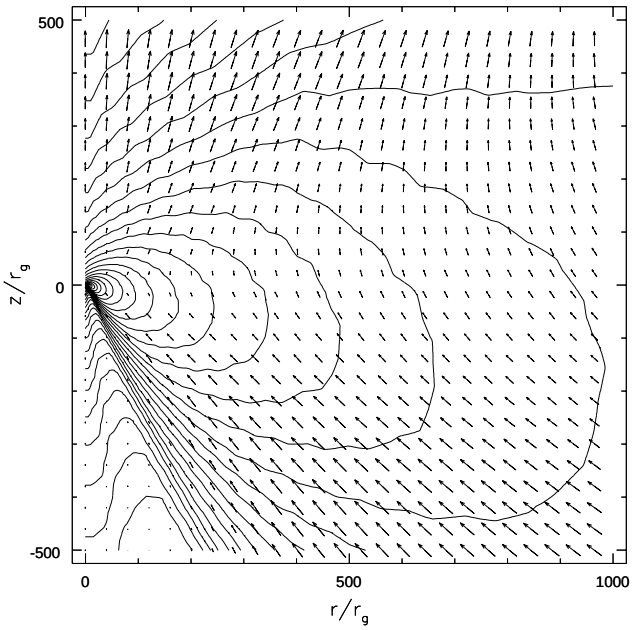

Figure 1. The flow pattern in Model B. Distributions of density ρ and the vector $r^2\rho\vec{v}$ are shown in the meridional cross section. The vertical axis coincides with the axis of rotation. The black hole is located in the origin (0,0). The contour lines are spaced with $\Delta \log \rho = 0.1$. Unipolar outflow is clearly seen in the vectors. Only a small fraction of the matter circulating in the computation domain directly accretes into the black hole.

The flow patterns with bipolar outflows in Models A and D are quite similar to those discussed by IA99 (their Models 1 and 5, respectively), despite differences in α and γ. The most interesting feature of Models B and C is the unipolar outflow. Figure 1 presents the flow pattern for Model B. Matter contained within the calculation domain forms a global meridional circulation cell with the spatial scale $\sim r_{out}$. Most of the stream-lines of the flow start at the source of matter at r_{out}, go inward, approach some minimum radius near to the equatorial plane, turn outward, and leave the computational domain through the upper hemisphere. In Model B we observe one large circulation cell (toroidal in three-dimensions), whereas in Model C the large circulation cell co-exists with a smaller one of opposite vorticity. The circulation is powered by the one-sided outflow generated in the vicinity of black hole. The part of the outflow which is close to the polar axis is most efficiently accelerated and becomes supersonic at a radial distance $\approx 1000r_g$. This part of the flow contains a small mass fraction and has outward directed velocities, which are larger than the escape velocity, $v_r > v_{esc} = \sqrt{2GM/r}$. Obviously, it can escape to infinity, even if cooling processes become efficient at large distances $r \gtrsim 1000r_g$. However, most of the outflowing matter forms a 'subsonic wind'. The evolution of this wind at large distances will be governed by cooling processes, which are not considered in our models.

What drives such powerful outflows and circulations? Obviously, the power is extracted from the rotating accretion flow with the help of a mechanism which redistributes energy

and momentum between different parts of fluid. In our non-radiative viscous models only the shear stress can provide such a mechanism. Due to the stress, the inner more rapidly rotating parts of the accretion flow pass a fraction of kinetic (not only rotational) energy to the outer parts.

The importance of outward energy transport supported by convection in geometrically thick accretion discs has been independently recognized by Bardeen (1973), Abramowicz (1974) and Bisnovatyi-Kogan & Blinnikov (1977), and first studied in detail by Paczyński & Abramowicz (1982) with a follow-up by Różyczka & Muchotrzeb (1982). However, these models do not include inward advection. In later works (Begelman & Meier 1982; Narayan & Yi 1995a; Honma 1996; Kato & Nakamura 1998; Manmoto et al. 2000) advection was included, but the convective outward energy flux was found to be weak, and was always dominated by the assumed purely inward directed advective energy flux. In the 'self-similar' models of ADAFs (Narayan & Yi 1994) the viscous energy flux,

$$\dot{E}_{visc}(r) = -2\pi r^2 \int_0^\pi (v_r \Pi_{rr} + v_\theta \Pi_{r\theta} + v_\phi \Pi_{r\phi}) \cos\theta d\theta, \quad (5)$$

is positive, directed outward, and is exactly balanced by the inward advection of energy with the corresponding flux

$$\dot{E}_{adv}(r) = 2\pi r^2 \int_0^\pi \rho v_r \left(\frac{v^2}{2} + W - \frac{GM}{r} \right) \cos\theta d\theta, \quad (6)$$

where W is the specific enthalpy. Thus, the total energy flux,

$$\dot{E} = \dot{E}_{adv} + \dot{E}_{visc}, \quad (7)$$

is zero everywhere, $\dot{E}(r) = 0$. Abramowicz, Lasota & Igumenshchev (1999) demonstrated that $\dot{E} = 0$ is an artifact of the assumed self-similarity: ADAFs that obey physically reasonable boundary conditions have, in general, $\dot{E} \neq 0$.

Our models have a specific geometry of flow which is very different from pure equatorial inflow. In Figure 2 we show the flow pattern for Model B in the vicinity of the inner boundary. In this figure the arrows show the velocity directions, and the ellipse is the projection of the radius $r = R_A$ at the equatorial plane. Matter, which crosses the equatorial plane inside R_A, accretes into the black hole at the rate $\dot{M}$. Using the analogy of the flow pattern in Figure 2 with Bondi-Hoyle accretion, we call R_A the 'accretion radius'. In the case of Model B, $R_A \approx 10 r_g$. Model C has a similar flow pattern, but R_A varies with time around the average value $\approx 80 r_g$.

The flow geometry shown in Figure 2 allows a significant transport of energy by shear stress from the matter accreted into the black hole to the matter outflowing to the upper hemisphere. Indeed, the stream lines of matter which is eventually inflowing and outflowing are located close together until the accreting matter reaches $r \sim R_A$. During this phase, efficient momentum and energy exchange takes place. We shall characterize the outward energy transport $\dot{E}$ by the 'accretion efficiency'

$$\epsilon = \dot{E}/\dot{M}c^2, \quad (8)$$

which is different from the standard definition of radiative efficiency,

$$\epsilon_{rad} = L/\dot{M}c^2, \quad (9)$$

where L is the total luminosity of accretion flow.

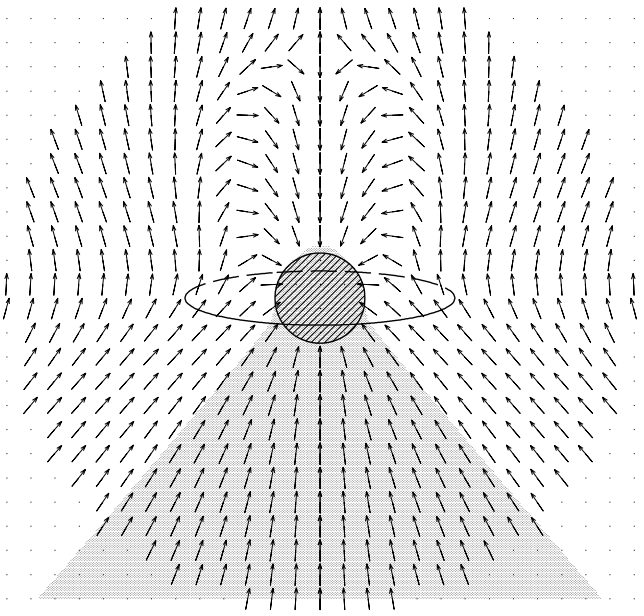

Figure 2. Two-dimensional structure of accretion flow in the innermost part of Model B. The region with radius $20 r_g$ is shown. The axis of symmetry of the picture coincides with the axis of rotation. The central shadow circle indicates the location of the inner numerical boundary. Arrows point to directions of motion. The ellipse is the projection of a circle of 'accretion' radius R_A at the equatorial plane. Matter, which crosses the equatorial plane inside R_A is absorbed by black hole. Regions with supersonic inward velocities are shown in grey.

Assuming that matter falls freely into the black hole inside R_A and that only the binding energy at the orbit $r = R_A$ is liberated, one can obtain an estimate of the maximum accretion efficiency,

$$\epsilon \simeq \frac{1}{4} \frac{r_g}{R_A}. \quad (10)$$

In the case of Models B and C, formula (10) predicts $\epsilon \approx 0.02$ and 0.004, respectively. Both values are significantly larger than the prediction of ϵ_{rad} for ADAFs, $\epsilon_{rad} \lesssim 10^{-4}$ (Narayan & Yi 1995b).

$\dot{E}(r)$, $\dot{E}_{adv}(r)$ and $\dot{E}_{visc}(r)$ for Model B are shown in Figure 3. In a steady state, $\dot{E}$ must be constant. The variation in $\dot{E}$ seen in Figure 3 is about 10%. This can be partially explained by a small non-stationarity of the flow, and small inaccuracies in our numerical code, which does not exactly conserve the total energy. Test calculations have shown that this inaccuracy gives an error of less than 5%. From Figure 3, one can see that for Model B, $\epsilon \approx 0.01$, which is only a factor of 2 smaller than what is predicted by estimate (10). The viscous flux $\dot{E}_{visc}$ (the dashed line in Fig.3) is always positive and dominates the advection flux $\dot{E}_{adv}$ (solid line) inside the radius $\approx 30 r_g$. At larger radii the energy is transported outward mainly by advection. Note, that $\dot{E}_{adv}$ changes sign at $r \approx 5 r_g$. Inside this radius the inward energy advection compensates a fraction of the outward viscous energy flux.

In all models, the time averaged net accretion rate $\dot{M}(r)$ through successive spheres of radius r, is a constant inside $\sim 1000 r_g$ to good accuracy. However, the rates of mass inflow $\dot{M}_{in}$ and outflow $\dot{M}_{out} = \dot{M}_{in} - \dot{M}$ are both increasing functions of r. In Model B $\dot{M}_{in}(r)$ is well approximated by a

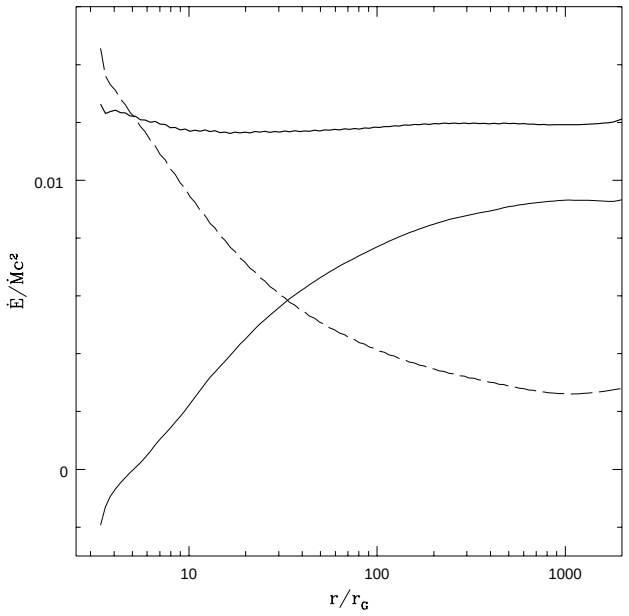

Figure 3. Radial dependence of the total energy flux $\dot{E}$ (heavy line), the advective energy flux $\dot{E}_{adv}$ (solid line) and the viscous energy flux $\dot{E}_{visc}$ (dashed line) in Model B. The energy fluxes are defined by eqs. (7), (6) and (5), respectively.

power law with index $\beta \approx 0.5$ in the radial range $10-1000r_g$. Models A, C and D show a similar power law behaviour for $\dot{M}_{in}(r)$, but with slightly different indices. Such a fast increase outward of $\dot{M}_{in}$ and $\dot{M}_{out}$ indicates the importance of global circulation motions in the dynamics of accretion flow in the models considered. Only a small part of the matter circulated in the computational domain is accreted by the black hole. Most of the matter in the case of (quasi) stable Models A, B and C, which starts at the source near to the outer boundary, has escaped outside the outer boundary after one cycle of circulation. This behaviour is in agreement with the results of Blandford & Begelman (1999), but unlike these authors, we see powerful outflows only in the case of large viscosity, $\alpha \gtrsim 0.1$. We also note that the radial dependence of $\dot{M}_{in}$ and $\dot{M}_{out}$ in our simulations is in good agreement with the results of Stone et al. (1999), although in thier models accretion flows are dominated by small-scale vortices and circulation motions.

4 DISCUSSION

Our numerical models can be applied to the two well-studied accretion regimes mentioned in the Introduction: optically thick and optically thin. The matter in optically thick flows is radiation dominated and characterized by $\gamma = 4/3$, so Models C and D can be relevant in this case. In optically thin flows the 'effective' adiabatic index ranges from about 3/2 to 5/3, depending on the strength of the magnetic field (see Narayan & Yi 1995b).

Flow patterns of 'optically thin' models consist of large-scale stable subsonic circulation cell(s) (in the $r-\theta$ plane): two equatorially symmetric cells in Model A and one cell in Model B. Only a small fraction of the outflowing matter forms the unbound supersonic unipolar outflow in Model B.

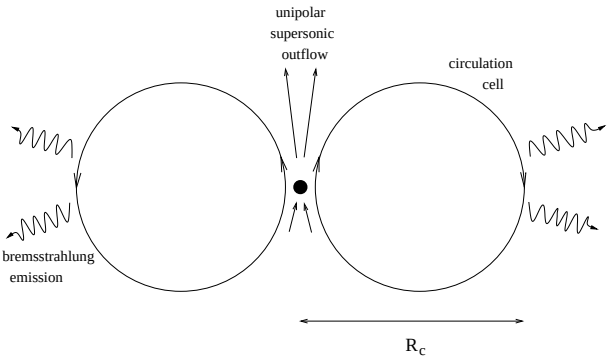

Figure 4. Schematic illustration of the proposed geometry of an optically thin rotating accretion flow accompanied by the global meridional circulation of matter.

A fraction $\epsilon \sim 0.01$ of the total energy of the matter accreted by the black hole is extracted and remains in the form of kinetic and thermal energy of the circulated matter. Although the present numerical models include no energy losses, one can speculate about the fate of subsonic outflows when energy losses are important, using the recent results obtained by Allen, Di Matteo & Fabian (1999) and Di Matteo et al. (1999). They have noted that in optically thin accretion flows coupled with strong outflows, the radiative energy losses are dominated by bremsstrahlung. The most efficient cooling in such accretion flows occurs at the maximum radius where this flow exists. Taking into account this result and the results of our numerical simulations we propose the following scenario of black hole accretion accompanied by global meridional circulation of matter. Subsonic outflows originate near to the black hole and are mainly supported by the pressure gradient force while the matter radiates weakly. At large radial distances, where the dynamical time scale of flows becomes comparable with the bremsstrahlung cooling time, the matter cools down and its outward motion cannot be supported any longer by the pressure gradient. The matter turns back and forms the inflowing part of the circulation cell(s). A schematic illustration of such a flow pattern in the case of one circulation cell near to the black hole is shown in Figure 4. Assuming that all of the thermal energy carried by outflows is radiated away, we can roughly estimate the radiative efficiency to be $\epsilon_{rad} \approx \epsilon \sim 0.01$. Note that this scenario can only be correct if the thermal instability develops slowly at the outer region of circulation cell(s), but this is what one would expect.

Basic properties of accretion flows with circulations can roughly be estimated. Let R_c be the spatial scale of the circulation cells which contain matter with the average density ρ_c. Comparing the bremsstrahlung cooling time for matter with the virial temperature and the dynamical time scale $t_d = R_c/V_c$ (where $V_c = \beta V_K$ is the mean circulation velocity at R_c, V_K is the Keplerian velocity and the value of the parameter $\beta \sim \alpha \sim 0.1$ is taken from numerical models), we can estimate $\rho_c \propto R_c^{-2}$ and consequently, the mass involved in circulations,

$$M_c \sim \left(\frac{\beta}{0.1}\right)\left(\frac{R_c}{10^3 r_g}\right)\left(\frac{M}{10^9 M_\odot}\right)^2 M_\odot, \qquad (11)$$

and the bremsstrahlung luminosity,

$$\frac{L}{L_{Edd}} \sim 3 \cdot 10^{-5} \left(\frac{\beta}{0.1}\right)^2 \left(\frac{10^3 r_g}{R_c}\right)^{3/2}. \quad (12)$$

Thus, the less massive and more compact object the higher luminosity it has. In a steady state, the external mass supply to the circulation cells is equal to the mass accretion rate $\dot{M} = L/\epsilon c^2$. Without the mass supply, the characteristic lifetime of the circulation cells is

$$t_c = \frac{M_c}{\dot{M}} \sim 10^3 \left(\frac{0.1}{\beta}\right) \left(\frac{\epsilon}{0.01}\right) \left(\frac{R_c}{10^3 r_g}\right)^{5/2} \left(\frac{M}{10^9 M_\odot}\right) \text{yrs.} \quad (13)$$

Note, that in estimates (11)-(13), we ignore the mass and energy losses due to the supersonic unipolar/bipolar outflows, and due to a wind which starts on the 'outer surface' of circulation cells and carries out all of the excess angular momentum.

Estimates (11) and (12) agree quite well with the observed data for the core of the elliptical galaxy M87 (Allen et al. 1999). Also, our finding of unipolar outflows from accreting black holes can be used to explain the one-sided jets observed in M87 and other objects.

Acknowledgments

We thank Marek Abramowicz and John Miller for stimulating discussions and comments on drafts of this paper. We gratefully acknowledge hospitality at the International School for Advanced Studies in Trieste, where a part of this work was done.

REFERENCES

Abramowicz M. A., 1974, Acta Astron., 24, 45
Abramowicz M. A., Jaroszyński M., Sikora M., 1978, A&A, 63, 221
Abramowicz M. A., 1981, Nature, 294, 235
Abramowicz M. A., Czerny B., Lasota J. P., Szuszkiewicz E., 1988, ApJ, 332, 646
Abramowicz M. A., Chen X., Kato S., Lasota J. P., Regev O., 1995, ApJ, 438, L37
Abramowicz M. A., Lasota J.-P., Igumenshchev I. V., 1999, MNRAS, submitted
Allen S. W., Di Matteo T., Fabian A. C., 1999, MNRAS, in press (astro-ph/9905052)
Bardeen J. M., 1973, in DeWitt C., ed., Black Holes. Gordon and Breach, New York, p. 241
Begelman M. C., 1978, MNRAS, 184, 53
Begelman M. C., Meier D. L., 1982, ApJ, 253, 873
Bisnovatyi-Kogan G. S., Blinnikov S. I., 1977, A&A, 59, 111
Blandford R. D., Begelman M. C., 1999, MNRAS, 303, L1
Di Matteo T., Quataert E., Allen S. W., Narayan R., Fabian A. C., 1999, MNRAS, in press (astro-ph/9905053)
Honma F., 1996, PASJ, 48, 77
Ichimaru C., 1977, ApJ, 214, 840
Igumenshchev I. V., Chen X., Abramowicz M. A., 1996, MNRAS, 278, 236
Igumenshchev I. V., Abramowicz M. A., 1999, MNRAS, 303, 309 (IA99)
Jaroszyński M., Abramowicz M. A., Paczyński B., 1980, Acta Astr., 30, 1
Kato S., Fukue J., Mineshige S., 1998, Black Hole Accretion Disks (Kyoto: Kyoto Univ. Press)
Kato S., Nakamura K., 1998, PASJ, 50, 559
Katz J. I., 1977, ApJ, 215, 265
Manmoto T., Kato S., Nakamura K. E., Narayan R., 2000, ApJ, in press
Narayan R., Yi I., 1994, ApJ, 428, L13
Narayan R., Yi I., 1995a, ApJ, 444, 231
Narayan R., Yi I., 1995b, ApJ, 452, 710
Narayan R., Mahadevan R., Quataert E., 1998, in Theory of Black Hole Accretion Disks, p. 148. Eds. M. A. Abramowicz, G. Björnsson, and J. E. Pringle (Cambridge: Cambridge Univ. Press)
Paczyński B., Abramowicz M. A., 1982, ApJ, 253, 897
Rees M. J., Phinney E. S., Begelman M. C. & Blandford R. D., 1982, Nature, 295, 17
Różyczka M., Muchotrzeb B., 1982, Acta Astron., 32, 285
Stone J. M., Pringle J. E., Begelman M. C., 1999, ApJ, in press
Xu G., Chen X., 1997, ApJ, 489, L29